CONF-9105144--4

DE91 017244

# INTERFEROMETRIC STUDIES FROM p–p–FRAGMENT COINCIDENCES

M. Korolija [1],[2], D. Shapira [3],[*], N. Cindro [1], J. Gomez del Campo [3],[*], H. J. Kim [3],[*], K. Teh [2] and J. Y. Shea [2],[4]

[1] Ruđer Bošković Institute, 41001 Zagreb, Croatia, Yugoslavia
[2] Joint Institute for Heavy Ion Research, Oak Ridge, TN-37831, USA
[3] Oak Ridge National Laboratory*, Oak Ridge, TN-37831, USA
[4] Department of Physics and Astronomy, Vanderbilt University, Nashville, TN-37235, USA

**Abstract**

Exclusive p-p correlations from the $^{58}$Ni + $^{58}$Ni reaction have been measured at an incident energy of 850 MeV. The enhancement in the p-p correlation function for small $\Delta p$ is satisfactorily explained by p-p final-state interaction effects. The observed enhancement is found to depend on the relative angle between the fragment and p-p c.m. velocities. The observed dependence of the p-p coincidence yield on the orientation of $\Delta$p with respect to the plane spanned by the fragment and p-p c.m. velocities is attributed to angular momentum effects.

## 1. Introduction

Light-particle correlations have been used quite extensively to obtain spatial and temporal information on the reaction zone from energetic heavy-ion collisions [1]. Intensity interferometry or the second-order interference effect was used by Hanbury-Brown and Twiss [2] to infer the size of distant stars by measuring photon-photon correlations with small relative momentum $\Delta p = (1/2)|p_2 - p_1|$ ($p_1$ and $p_2$ are momenta of the two coincident photons). In nuclear physics, Goldhaber, Goldhaber, Lee and Pais [3] were the first to apply the same technique to estimate the particle-production region in relativistic p-$\bar{p}$ collisions.

As is well known, there is no final-state interaction between emitted photons. This, however, is not the case for emitted particles, where the final-state interaction causes additional complications. As an example, let us take p-p correlations since we are interested mostly in these correlations. In the case of stochastic two-proton emission there is an interplay of Coulomb, statistical and nuclear effects in the final

state [4,5]. Positive correlations at small $\Delta p$ result from the dominance of the attractive nuclear force (in the S state) over the combined effect of the repulsive Coulomb force and unfavorable (Fermi) statistics.

According to the models from refs. 4-5 the p-p correlation function yields information on both the source size ($r_0$) and the lifetime ($\tau$) through an effective source size $\rho = [r_0^2+(v_{rel}\cdot\tau)^2]^{1/2}$; $v_{rel} = |\mathrm{v_{pp}} - \mathrm{v_f}|$ is the velocity of the c.m. of the emitted pair of particles ($\mathrm{v_{pp}} = (1/2m_p)(\mathrm{p_1} + \mathrm{p_2})$; $m_p$ is the proton mass) relative to the fragment (source) velocity ($\mathrm{v_f}$). Since in the intermediate energy range light-particle-emission times are typically of the order of $10^{-22} - 10^{-21}$ s, the contribution of the term $v_{rel}\cdot\tau$ to the effective source size $\rho$ cannot be neglected. In fact, for sufficiently large emission times $\tau$, it can even account for the whole effect. Obviously, $\rho$ approaches $r_0$ in the limit $v_{rel} \rightarrow 0$; this condition is met in exclusive measurements only.

## 2. Experiment

Exclusive $p$-$p$ correlations from the $^{58}$Ni + $^{58}$Ni reaction were measured using the HILI detection system [6] at the Holifield Heavy Ion Research Facility of the Oak Ridge National Laboratory. A 1 mg/cm$^2$ $^{58}$Ni target was bombarded with an 850-MeV $^{58}$Ni beam. The charge, energy, and direction of the heavy fragment were obtained from a position-sensitive ionization chamber. Protons were detected using an array of 96 $\Delta E - E$ phoswich scintillator detectors [7].

The correlation function R was calculated from the expression

$$R(\mathrm{p_1}, \mathrm{p_2}, \mathrm{p_f}) + 1 = \frac{\sigma_{123}(\mathrm{p_1}, \mathrm{p_2}, \mathrm{p_f})}{\sigma_{123}{}'(\mathrm{p_{1,1}}, \mathrm{p_{1,2}}, \mathrm{p_{1,f}}; \mathrm{p_{2,1}}, \mathrm{p_{2,2}}, \mathrm{p_{2,f}})} \quad , \tag{1}$$

where $\sigma_{123}(\mathrm{p_1}, \mathrm{p_2}, \mathrm{p_f})$ is the measured yield of triple coincidence events consisting of two protons with momenta $\mathrm{p_1}$ and $\mathrm{p_2}$ and a fragment with momentum $\mathrm{p_f}$ and $\sigma_{123}{}'$ $(\mathrm{p_{1,1}}, \mathrm{p_{1,2}}, \mathrm{p_{1,f}}; \mathrm{p_{2,1}}, \mathrm{p_{2,2}}, \mathrm{p_{2,f}})$ the background yield of triple coincidences with particles stemming from two different events (first set of indices). $\sigma_{123}{}'$ was constructed by selecting for the background yield events of the same class as in $\sigma_{123}$ [8], (same number of coincident particles), which satisfied the conditions

$$|\theta_{1,f} - \theta_{2,f}| \leq 1^\circ, \quad |\phi_{1,f} - \phi_{2,f}| \leq 4^\circ, \quad |E_{1,f} - E_{2,f}| \leq 10\ MeV, \tag{2}$$

where $\theta_f$ and $\phi_f$ are the fragment polar and azimuthal angles and $E_f$ is the fragment kinetic energy. The indices 1 and 2 refer to the two different events. The total background yield $\sigma_{123}'$ was obtained by treating each measured event on an equal footing, i.e., by taking into account all possible combinations of the measured events.

## 3. Results and Discussion

The p-p correlation functions for fragments in the charge range $21 \leq Z \leq 26$ are shown in Figs. 1 (a)-(b) for two different geometries (see top of the figure). Fig. 1(a) shows the p-p correlation function obtained for a geometry where all the three particles were detected above the beam axis (geometry I). Similarly, Fig. 1(b) shows the p-p correlation function for a configuration where the two light particles are detected above and the heavy fragment below the beam axis (geometry II). Also, the two p-p correlation functions are given for data with (open symbols) and without (full symbols) a gate on the relative velocity $v_{rel}$. In calculating $v_f$ from $p_f$, for the mass of each fragment of given charge Z we have taken the most probable mass obtained from a mass distribution calculated with the statistical evaporation code LILITA [9].

The distributions of $v_{rel}$ for the two geometries are shown in Figs. 2(a) and (b), respectively. The shaded areas refer to the data obtained by setting a gate $v_{rel} \leq 0.072\ c$ on the data. Fig. 3 shows proton (a) and heavy-fragment (b) spectra which correspond to the $v_{rel}$ spectra shown in Fig. 2(a) and, also, to the p-p correlation functions shown in Fig. 1(a). This figure shows the effect of selecting events with small $v_{rel}$. Assuming the binary reaction in the incident channel, the "gate-on" and "no-gate" data shown in Fig. 3(b) overlap in a substantial range of fragment excitation energy around $E^* \simeq 100$ MeV ($E_f \simeq 650$ MeV). In what follows we shall relate the extracted (fragment) source size and lifetime to this range of the excitation energy. In doing so, the mean source size is assumed to be constant and spherical throughout the course of the reaction.

The determination of the source size $r_0$ and its lifetime $\tau$ proceeds in the following way. The measured p-p correlation functions were compared with the calculations performed using the model from Ref. 4 which includes the p-p final-state interaction. In the calculations the finite resolution of the $\Delta E - E$ hodoscope elements was taken

into account. The measured p-p correlation functions for $\Delta p$ projected in the $v_{rel}$ direction ($\Delta p_{\parallel}$) and the corresponding results of the calculation obtained by taking $\Delta p_{\perp} = 0$ are shown in Fig. 4. Such a presentation has been chosen in view of the fact that the p-p correlation function projected in the $v_{rel}$ direction is highly sensi-

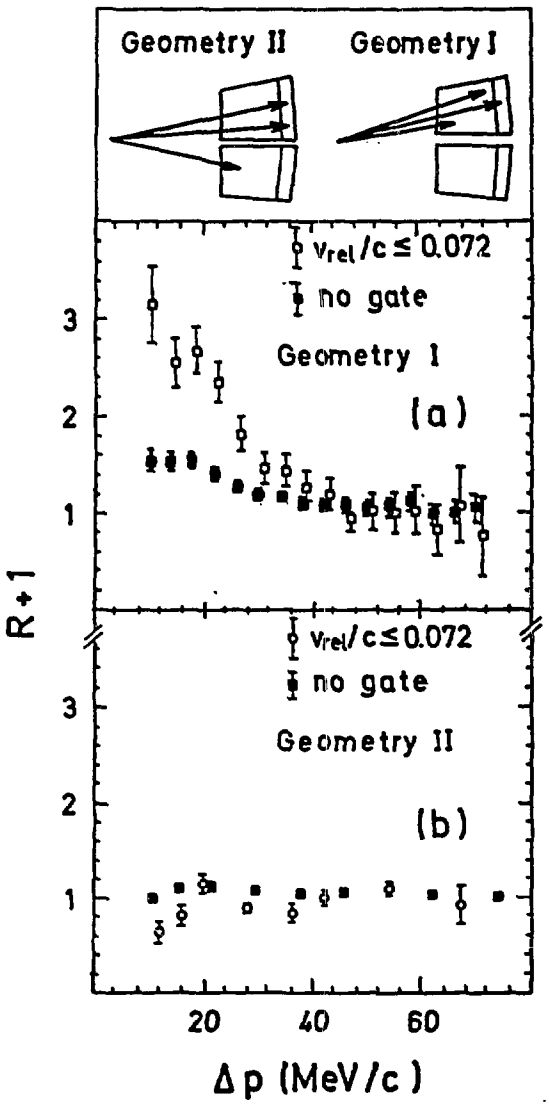


Fig. 1. Proton correlation functions for the $^{58}Ni + ^{58}Ni$ reaction at an incident energy of 850 MeV for two different experimental arrangements shown on the top. The proton correlation functions with a gate on the data (open symbols) and with no gate on $v_{rel}$ (full symbols) are shown for geometry I (a) and geometry II (b). Error bars give statistical uncertainties only.

tive to the lifetime effects [10]. Open squares correspond to the p-p correlation function obtained with a gate on $v_{rel}$, while full squares correspond to that obtained

with no gate on the data. The lines refer to the calculated values obtained following Ref. 4 by taking $r_0$=2.7 fm and varying $v_{rel}\cdot\tau$ in the range 9 ± 2 fm (Fig. 4(a)) and 18 ± 2 fm (Fig. 4(b)).

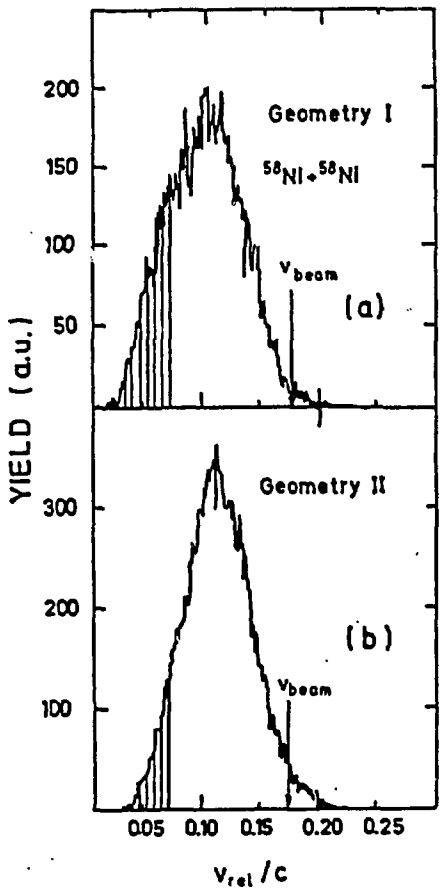


Fig. 2. Distribution of $v_{rel}$ for (a) geometry I and (b) geometry II.

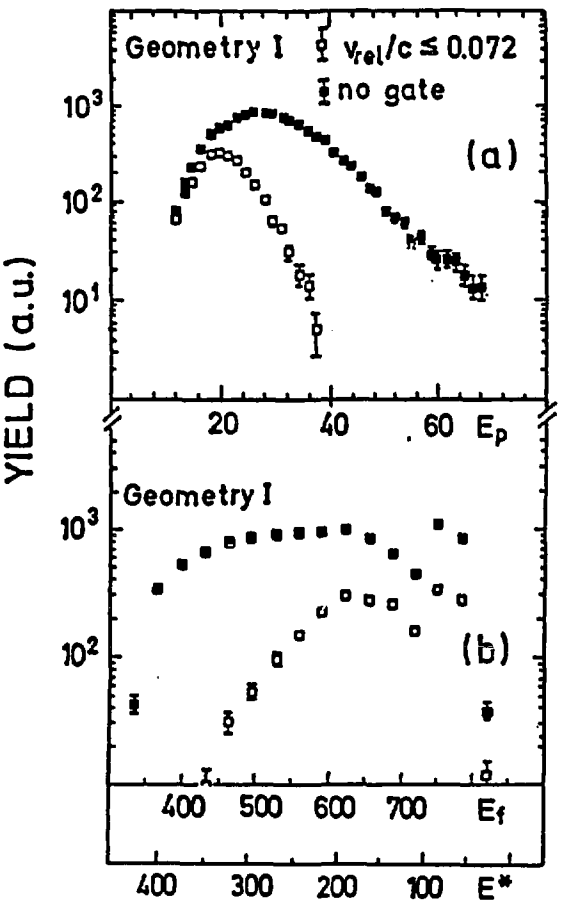


Fig. 3. Proton (a) and fragment (b) kinetic energy spectra for geometry I. Symbols are as in Fig. 1(a). The abscissa (energy) is in MeV.

The best-fit values of the source size ($r_0$) and the lifetime ($\tau$) were determined using the following procedure. First, the p-p correlation function measured for the data with a gate on $v_{rel}$ (open squares) were fitted by the calculations. This yielded values of the source size of 2.7 fm and of the parameter $v_{rel}\cdot\tau$ of 9 ± 2 fm. Then,

assuming a constant source size of 2.7 fm, a value of the parameter $v_{rel} \cdot \tau = 18 \pm 2$ fm was obtained from the fit to the p-p correlation function for the data with no gate on $v_{rel}$ (full squares). The average value of the lifetime $\tau$ was then determined by taking for $v_{rel}$ an average of the values of $v_{rel}$ shown in Fig. 2(a). For the gate-on condition, we obtain $<v_{rel}> = 0.06$ c; while for the no gate condition, $<v_{rel}> = 0.10$ c. Introducing these values into the obtained best-fit values for $v_{rel} \cdot \tau$, we obtain source-lifetime values $(3.9 \leq \tau \leq 6.1) \times 10^{-22}$ s and $(5.3 \leq \tau \leq 6.6) \times 10^{-22}$ s for the gate-on and no-gate conditions, respectively. The obtained values of $\tau$ show a remarkable consistency.

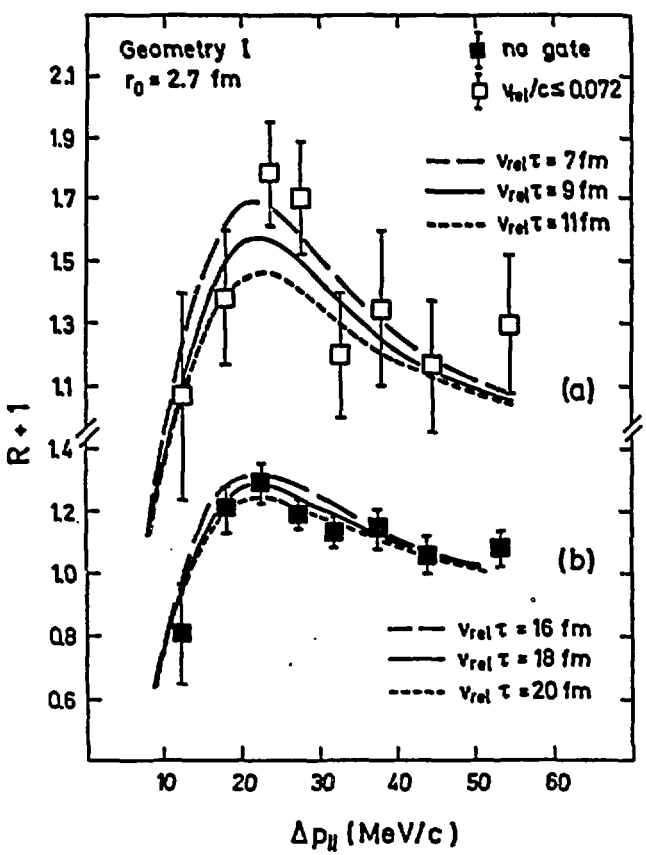


Fig. 4. Proton correlation functions vs. the value of $\Delta p$ projected on the $v_{rel}$ axis ($\Delta p_{\parallel}$) for $^{58}Ni + ^{58}Ni$ for geometry I. Lines show calculations of the p-p correlation function obtained using the model of Ref. 4, for $\Delta p$ parallel to $v_{rel}$. Symbols are as in Fig. 1(a).

Correlated light particles can also stem from the decay of resonances. To estimate this contribution to the measured p-p correlation function, we have used the

thermodynamical statistical model [11]. In this model, the production of the unstable fragment $^2$He is followed by its subsequent decay into a correlated p-p pair. The contribution of this process for geometry I was estimated with the help of the Hauser-Feshbach program BUSCO [12]. In this calculation angular ($\Delta\theta_{pp} = \pm 3°$) and momentum ($\Delta p = 20 \pm 3$ MeV/c) constraints were applied. Taking into account the actual solid angle covered by the HILI detector and taking for $^{58}$Ni an excitation energy $E^* = 150$ MeV and an angular momentum of $J_{max} = 50\ \hbar$, we have obtained a factor of $\simeq 10^2$ in favour of 2 p vs. $^2$He emission.

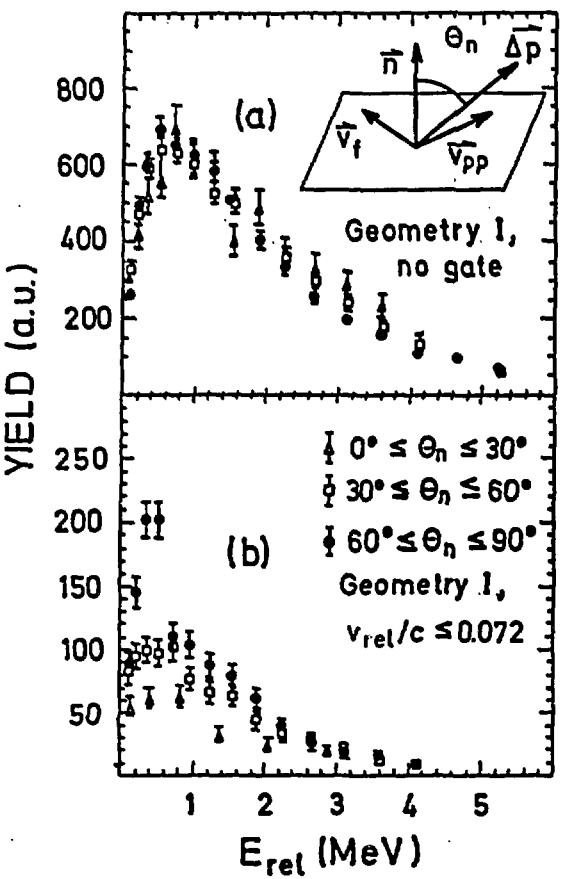


Fig. 5. Total p-p coincidence yield for $^{58}$Ni + $^{58}$Ni data with no gate (a) and with a gate on $v_{rel}$ (b) for geometry I. Symbols in both figures refer to total triple coincidence yields for the $\theta_n$ slices shown in (b).

In the final-state interaction model of Ref. 4 the influence of the angular momentum on p-p correlations has not been investigated. On the other hand, the influence of

angular momentum effects on n-n correlations was discussed in Ref. 13, where it was shown that the n-n correlation function is, in fact, sensitive to angular-momentum effects. In this model, neutrons were assumed to originate from the rapidly spinning compound nucleus. Although the n-n final-state interaction is not included in the model, we expect a similar dependence when final-state interaction effects are taken into account.

In this respect, Figs. 5 (a)-(b) show the dependence of the total p-p coincidence yield on the direction of $\Delta \mathbf{p}$ relative to the plane spanned by the vectors $\mathbf{v_{pp}}$ and $\mathbf{v_f}$ (see inset). The angle $\theta_n$ is the angle between the normal n on this plane and $\Delta \mathbf{p}$. As can be seen from Fig. 5(a), the p-p coincidence yield averaged over the whole $v_{rel}$ distribution shows no dependence on the particular slice of $\theta_n$. On the other hand, the p-p coincidence yield with a gate on $v_{rel}$ (Fig. 5(b)) shows a different pattern. The enhancement in the p-p coincidence yield at small values of $E_{rel}$ corresponds to such events where all the three vectors, $\mathbf{v_f}$, $\mathbf{v_{pp}}$ and $\Delta \mathbf{p}$, are essentially coplanar ($60° \leq \theta_n \leq 90°$). The strong dependence of the p-p correlation function on the orientation of $\Delta \mathbf{p}$, observed in this work, suggests the necessity of including angular momentum effects into the p-p final-state interaction theory.

## 4. Conclusions

In summary, the measured p-p correlation function for the $^{58}$Ni + $^{58}$Ni reaction at $E_{inc}$ = 850 MeV shows a strong enhancement for small values of $\Delta p$. The observed enhancement is interpreted as a result of the interaction of the emitted protons in the final-state. Interpreting this enhancement as a result of the production and subsequent decay of the unstable resonance $^2$He, is ruled out on the grounds that the expected production of $^2$He is small for the range of the fragment excitation energy analyzed in this work. The p-p correlation function has been found to decrease very rapidly with the increase of the relative angle between the fragment and the two-proton c.m. velocities. The enhancement in the p-p correlation function observed when all the particle velocity vectors are coplanar is interpreted as a result of angular momentum effects.

This paper is part of a study under the US-Yugoslav collaboration project JF 939 DOE/IRB.

(*) ORNL is operated by Martin Marietta Energy Systems, Inc., under contract No. DE-AC05-840R21400 with the U.S. Department of Energy.

## References

[1] D.H. Boal, C.K. Gelbke and B.K. Jennings, Rev. of Mod. Phys. 62 553 (1990) and references cited therein.

[2] R. Hanbury-Brown and R. Q. Twiss, Nature (London) 178 1046 (1956).

[3] G. Goldhaber, S. Goldhaber, W. Lee and A. Pais, Phys. Rev. 120 300 (1960).

[4] S.E. Koonin, Phys. Lett. B70 43 (1977).

[5] R. Lednicky and V.L. Lyuboshits, Yad. Fiz. 35 1316 (1982); Sov. J. Nucl. Phys. 35 770 (1982).

[6] D. Shapira, K. Teh, J. Blankenship, B. Burks, L. Foutch, H. J. Kim, M. Korolija, J. W. McConnell, M. Messick, R. Novotny, D. Rentsch, J. Shea and J. P. Wieleczko, Nucl. Instrum. & Methods A301 76 (1991).

[7] K. Teh, D. Shapira, J. W. McConnell, H. J. Kim and R. Novotny, IEEE Tran. in Nucl. Science 35 272 (1988).

[8] W.A. Zajc, J.A. Bistirlich, R.R. Bossingham, H.R. Bowman, C.W. Clawson, K.M. Crowe, K.A. Frankel, J.G. Ingersoll, J.M. Kurck, C.J. Martoff, D.L. Murphy, J.O. Rasmussen, J.P. Sullivan, E. Yoo, O. Hashimoto, M. Koike, W.J. McDonald, J.P. Miller and P. Truöl, Phys. Rev. C29 2173 (1984).

[9] J. Gomez del Campo and R. Stokstad, ORNL Report No. TM7295 1981 (unpublished).

[10] S. Pratt and M.B. Tsang, Phys. Rev. C36 2390 (1987).

[11] W.A. Friedman and W.G. Lynch, Phys. Rev. C28 16 (1983); M.A. Bernstein, W.A. Friedman and W.G. Lynch, Phys. Rev. C29 132 (1984).

[12] J. Gomez del Campo, J.L. Charvet, A. D'Onofrio, R.L. Auble, J.R. Beene, M.L. Halbert and H.J. Kim, Phys. Rev. Lett. **61** 290 (1988).

[13] S.E. Koonin, W.A. Bauer and A. Schäfer, Phys. Rev. Lett. **62** 1247 (1989).